REPORT DOCUMENTATION PAGE

Form Approved
OMB No. 0704-0188

AGENCY USE ONLY (Leave blank)	2. REPORT DATE	3. REPORT TYPE AND DATES COVERED
	April 29, 1994	Final Report, 2/1/91 - 3/31/94

TITLE AND SUBTITLE
High-Intensity and High Energy Laser Interactions with Single Droplets

5. FUNDING NUMBERS
DAAL03-91-G-0042

AUTHOR(S)
Richard K. Chang

PERFORMING ORGANIZATION NAME(S) AND ADDRESS(ES)
Department of Applied Physics
Yale University
P.O. Box 208284
New Haven, CT 06520-8284

8. PERFORMING ORGANIZATION REPORT NUMBER

9. SPONSORING/MONITORING AGENCY NAME(S) AND ADDRESS(ES)
U. S. Army Research Office
P. O. Box 12211
Research Triangle Park, NC 27709-2211

10. SPONSORING/MONITORING AGENCY REPORT NUMBER
ARO 28489.11-GS

11. SUPPLEMENTARY NOTES
The view, opinions and/or findings contained in this report are those of the author(s) and should not be construed as an official Department of the Army position, policy, or decision, unless so designated by other documentation.

12a. DISTRIBUTION/AVAILABILITY STATEMENT
Approved for public release; distribution unlimited.

12b. DISTRIBUTION CODE

13. ABSTRACT *(Maximum 200 words)*

Our research accomplishments have been in five main areas: (1) Third-order sum frequency generation in the volume of the droplet and the role of phase-matching condition with droplet-cavity modes which are standing waves; (2) Retention of acoustic phonons generated by stimulated Brillouin scattering (SBS) and the role of these long-lived acoustic waves and photons in "seeding" the SBS during the subsequent input-laser pulse; (3) Stimulated low-frequency scattering from anisotropic molecules in droplets and the effect of the low-frequency scattering process in causing the elastic scattering spectrum and the stimulated Raman scattering (SRS) spectrum to be asymmetrically broadened; (4) Resonance Raman enhancement of the SRS gain coefficient with the intent to increase the sensitivity of SRS to minor species in the droplet; and (5) The use of population-inverted laser-dye molecules to provide "extra" gain for SRS from minor species in the droplet.

14. SUBJECT TERMS
Nonlinear Optics, Droplets, Microcavity, Phase-matching Condition, Stimulated Brillouin Scattering, Stimulated Raman Scattering, Resonance Raman Scattering, Lasing Media, and Dye Fluorescence.

15. NUMBER OF PAGES
21

16. PRICE CODE

17. SECURITY CLASSIFICATION OF REPORT	18. SECURITY CLASSIFICATION OF THIS PAGE	19. SECURITY CLASSIFICATION OF ABSTRACT	20. LIMITATION OF ABSTRACT
UNCLASSIFIED	UNCLASSIFIED	UNCLASSIFIED	UL

NSN 7540-01-280-5500

Standard Form 298 (Rev. 2-89)
Prescribed by ANSI Std. Z39-18
298-102

High-Intensity and High-Energy Laser Interactions with Single Droplets

Final Report

Richard K. Chang

April, 1994

U. S. Army Research Office

Contract No: DAAL03-91-G-0042
(February 1, 1991 - March 31, 1994)

Yale University
Department of Applied Physics and Center for Laser Diagnostics
P. O. Box 208284
New Haven, Connecticut 06520-8284

Approved for public release;
Distribution unlimited.

The view, opinions and/or findings contained in this report are those of the author and should not be construed as an official Department of the Army position, policy, or decision, unless so designated by other documentation.

CONTENTS

Introduction

Our research goals during the past three years and two months have been directed toward further understanding of nonlinear optical interactions within single droplets which are irradiated with a single or a train of high-intensity laser pulses. In the visible-UV regions, there are three features unique to micrometer-sized droplets: (1) High concentration of the input-laser intensity inside the droplet; (2) Large enhancements of the inelastic scattering cross section; and (3) Large Q values for the optical feedback provided to the internally generated nonlinear waves. Because of these three features, nonlinear optical effects are readily generated within the droplets, which are irradiated by high-intensity laser pulses. The main objective is to extend our knowledge of nonlinear optics from a conventional liquid cell to single droplets and eventually to a spray.

Our research accomplishments have been in five main areas: (1) Third-order sum frequency generation in the volume of the droplet and the role of phase-matching condition with droplet-cavity modes which are standing waves; (2) Retention of acoustic phonons generated by stimulated Brillouin scattering (SBS) and the role of these long-lived acoustic waves and photons in "seeding" the SBS during the subsequent input-laser pulse; (3) Stimulated low-frequency scattering from anisotropic molecules in droplets and the effect of the low-frequency scattering process in causing the elastic scattering spectrum and the stimulated Raman scattering (SRS) spectrum to be asymmetrically broadened; (4) Resonance Raman enhancement of the SRS gain coefficient with the intent to increase the sensitivity of SRS to minor species in the droplet; and (5) The use of population-inverted laser-dye molecules to provide "extra" gain for SRS from minor species in the droplet.

Research Accomplishments

A brief review of each of these five areas will follow. All of the research results have been published. See List of Publications on page 18. Each of the publications have been submitted as Technical Reports.

(a) Third Harmonic Generation

In an earlier ARO-funded research period (February 1, 1988- January 31, 1991 DAAL03-88-K-0040) we reported on the generation (THG) and third-order sum frequency generation (TSFG) in droplets. During the present ARO-funded grant period, the overall aim of this portion of our investigation was to understand the phase-matching condition for nonlinear parametric processes (commonly referred to as four-wave-mixing processes) in droplets. Because of the isotropic symmetry of the liquid, the second-order optical susceptibility $\chi^{(2)}$ is zero in the electric dipole approximation. Hence, there is no volume second-order sum frequency generation (such as SHG) in the interior of droplets. However, the third-order optical susceptibility $\chi^{(3)}$ of a liquid is not zero. TSFG from droplets results from the nonlinearly generated polarization $P^{NLS}(\omega_{TSFG})$ inside the droplet, where $P^{NLS}(\omega_{TSFG}) = \chi^{(3)}E(\omega_1)E(\omega_2)E(\omega_3)$ and $E(\omega_i)$ is the electric field amplitude at ω_i inside the droplet. Energy conservation requires $\omega_{TSFG} = \omega_1 + \omega_2 + \omega_3$, where ω_i can be the frequency of the input laser at ω_L or the frequencies of the jth-order Stokes SRS at $\omega_{js} = \omega_L - j\omega_{vib}$. The vibrational frequency of the molecule in the liquid is ω_{vib}. Figure 1 shows that the detected multiorder Stokes SRS of CCl_4 droplets can extend to $j = 20$ and beyond, had it not been for the detector sensitivity decrease in the near infrared. Consequently, the various $E(\omega_{js})$'s can generate $P^{NLS}(\omega_{TSFG})$, resulting in discrete TSFG peaks with intensity $I_{TSFG}(p)$ at frequencies $\omega_{TSFG}(p) = 3\omega_L - p\omega_{vib}$, where p is an integer and can vary from $p = 0$ (for THG of ω_L) to a maximum value of $p = 3j$ (for THG of ω_{js}). However, Fig. 2 shows that at any fixed droplet radius (or at a fixed oscillation frequency of the droplet generator f_{osc}) only a few $I_{TSFG}(p)$ peaks are detectable. When the droplet radius or f_{osc} is changed, Fig. 2 shows that a few different $I_{TSFG}(p)$ peaks are detected. The experimental observation of a few $I_{TSFG}(p)$ peaks and the sensitivity of the TSFG spectra to droplet radius suggested that some form of phase-matching requirement is playing a role in droplets. [For more details see Publication A].

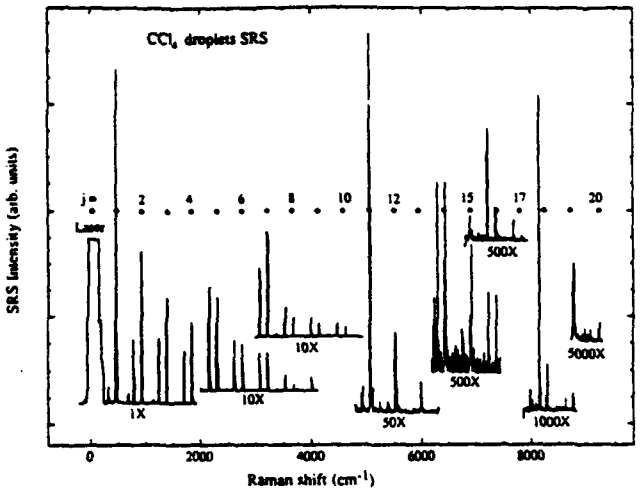

Figure 1. Detected SRS spectra from CCl_4 droplets plotted as a function of the Raman shift from the input-laser frequency. The integer j (above the points) corresponds to the SRS frequency $\omega_{js} = \omega_L - j\omega_{vib}$, where $\omega_{vib} = 459\ cm^{-1}$ is the vibrational frequency of the ν_1 mode of CCl_4. Cascade multiorder Stokes SRS up to j = 20 is detected before the near-infrared sensitivity of the detector significantly decreases. Combinations and overtones of the ν_2 and ν_4 vibrational modes are also detected. The incident laser wavelength is $\lambda_L = 0.532\ \mu m$ and the detector is a CCD. [From Publication A].

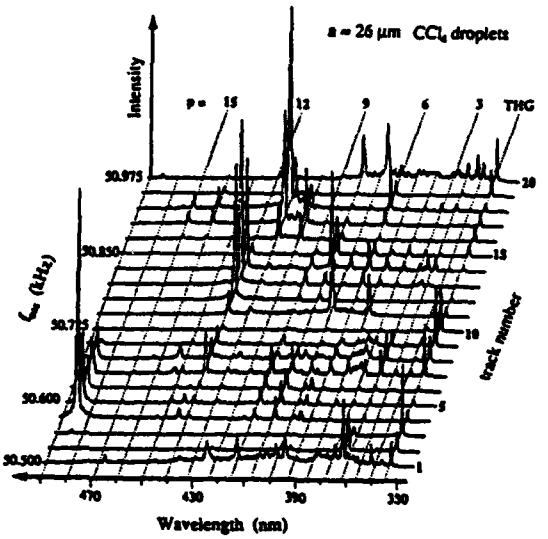

Figure 2. Detected TSFG Spectra from CCl4 droplets as 20 consecutive f_{osc} (shown on the vertical abscissa) at 25 Hz increments. The horizontal abscissa indicates wavelength decreasing toward $\lambda_L/3$, and the series of dotted lines corresponds to $\omega_{TSFG}(p) = 3\omega_L - p\omega_{vib}$, where p is an integer that ranges from p = 0 to p = 3x(the highest j-th multiorder Stokes SRS). The incident wavelength is $\lambda_L = 1.064\ \mu m$ and the detector is a position-sensitive resistive-anode device, Mepsicron. [From Publication A].

For TSFG in a liquid cell excited by plane waves, the phase-matching condition is a result of spatial overlap in the propagation direction z;

$$\int [\exp(\vec{k}_{TSFG}-\vec{k}_1-\vec{k}_2-\vec{k}_3)\,\vec{z}\,]dz \qquad (1)$$

In a liquid droplet, the internal waves are no longer plane waves. The input laser radiation at ω_L is highly distorted by the droplet-air interface. A standing wave results only if ω_L is on a droplet-cavity resonance, commonly referred to as a morphoplogy-dependent resonance MDR. The SRS radiation at ω_{js} is always on a MDR, since the generation of the various multiorder Stokes SRS requires optical feedback provided by the MDR. Consequently, the internal field distribution of SRS always mimics the field distribution of a MDR while the internal field distribution at ω_L mimics the field distribution of a MDR only if ω_L is on an input resonance with a MDR.

With the collaboration of Dr. Steven C. Hill [a NCR Research Associate at the Atmospheric Sciences Laboratory, White Sands Missile Range, New Mexico], we established that the phase-matching conditon of plane waves in a liquid cell [see Eq. (1)] is equivalent to spatial overlap of the field distributions of $P^{NLS}(\omega_{TSFG})$ and of the three $E(\omega_i)$'s, integrated throughout the volume of the sphere. In order to increase the interaction length among the four waves, ω_{TSFG} must be on a MDR. Furthermore, in order to have a detectable $I_{TSFG}(\omega_{TSFG})$, the $P^{NLS}(\omega_{TSFG})$ and three $E(\omega_i)$'s must be on MDR's that have large spatial overlaps. Because the field distributions of the MDR's can be both + and -, only a few spatial overlap integrals of four MDR's can be large for a droplet with a fixed radius and hence, only a few discrete combinations of frequencies $\omega_{TSFG}(p) = 3\omega_L - p\omega_{vib}$ can give rise to detectable $I_{TSFG}(\omega_{TSFG})$ peaks. [For more details see Publication B].

The realization that spatial overlaps of $P^{NLS}(\omega_{TSFG})$ and the three $E(\omega_i)$'s are equivalent to the phase-matching requirement of plane waves in an optical cell can be generalized to other four-wave mixing processes, such a coherent anti-Stokes Raman scattering and coherent Raman gain. In fact, the spatial overlap concepts developed for

waves circulating in droplets can be also applied to three-wave mixing processes (such as SHG and SFG) in the interior of the droplet.

(b) Retention of Acoustic Phonons

Stimulated Brillouin scattering (SBS) at ω_{SBS} is associated with the parametric interaction of the incident laser radiation at ω_L with coherently driven acoustic waves that are nonlinearly generated by the "beating" of the $E(\omega_L)$ and $E^*(\omega_{SBS})$ through the electrostriction effect. The frequency of the acoustic phonons ω_{ac} is related to the $\vec{q}$ as follows: $\omega_{ac} = v_s |\vec{q}|$, where v_s is the acoustic wave speed in the liquid, $|\vec{q}| = 2|\vec{k}_L|\sin(\theta/2)$, $\vec{k}_L$ is the wave vector of the incident light, and θ is the angle between the input-laser wave with $\vec{k}_L$ and the SBS wave with $\vec{k}_{SBS}$. The Brillouin phonon decay rate $G_{ac}(q)$ is dependent on $|\vec{q}|$, i.e., $G_{ac}(q) = G|q|^2$, where G is the damping parameter. The phonon decay time $T_2 = [G_{ac}(q)]^{-1}$ is the shortest for the backward propagating SBS, where $\theta \approx 180°$ or $|q| \approx 2|\vec{k}_L|$. For CCl_4 in an optical cell, $T_2 \approx 1$ ns for backward SBS (with $\theta \approx 180°$). For near-forward SBS (with $\theta \approx 4°$), T_2 can be some two-orders of magnitude longer , e.g., $T_2 \approx 200$ nsec.

In an earlier ARO-funded research period, we have observed SBS, by using a 7 nsec duration laser pulse, from the second harmonic output of a Q-switched Nd:YAG laser, to illuminate the droplets and a Fabry-Perot interferometer to measure the frequency shift $[\Delta\omega = (\omega_L - \omega_{SBS}) = \omega_{ac}]$ of the SBS from the input-laser frequency. At that time, we concluded that large wavevector $\vec{q}$ (with $\theta \approx 180°$ and $\theta \approx 90°$) acoustic waves are generated.[3] The maximum $\Delta\omega$ is less than 0.7 GHz from the green input-laser radiation. When the temporal responses of the SBS and SRS were measured simultaneously, we noted[4] that the SBS reaches threshold before the SRS and that there exists a temporal correlation between the decay of the SBS and the growth of the SRS[4]. It is the SBS and not the input laser radiation that pumps the SRS and the SBS eventually becomes depleted. Subsequently, more input-laser radiation must again pump the SBS, which eventually becomes depleted again[4]. To our surprise, we noted that the SBS emerging from the

droplet (at 90° with respect to the input-laser beam direction) was much more intense than the normal 90° elastic scattering. We have not quantified the ratio of green scattering at high and low input-laser intensities.

During the present ARO-funded grant period, we did not expect to observe any SBS from droplets illuminated with a train of pulses (having a interval of 13.2 nsec) with pulse duration Δt_p = 100 psec emerging from the second harmonic output of a mode-locked Nd:YAG laser. When $\Delta t_p < T_2$, the well accepted view is that the transient Brillouin gain is approximately reduced from the steady-state Brillouin gain by $\Delta t_p/T_2$, which is 1/10 for backward SBS and 1/2000 for near-forward SBS. Figures 3 and 4 show the unexpected 90° detected green "elastic" scattering results when a single CS_2 droplet and a single CCl_4 droplet are illuminated with a train of mode-locked pulses with Δt_p = 100 psec. The word elastic is in quotes to designate that both the green elastic scattering and the green SBS were detected, but not spectrally resolved with an interferometer. At high input-laser intensities, the 90° scattered intensities from the first few input-laser pulses are lower than those from the third and subsequent input-laser pulses. At low input-laser intensities, the 90° scattered intensities mimic the input-laser intensities. We also noted that when the 100 psec laser beam is focused at the droplet edge, the intense green SBS is noted to emerge from one droplet edge, commensurate with near-forward SBS. However, when the 7 nsec laser beam is focused at the droplet edge, the intense green SBS is noted to emerge from the opposite droplet edge, commensurate with backward SBS. [For more details see Publication C].

We have not made any measurements pertaining to the single-ended lidar configuration, where the laser and detector are at the same end. Normally, in the single-end measurements only the 180° backward SBS from the atmosphere plays a role. However, because of the droplet morphology which causes the internally generated SBS to circulate within the droplet, both the backward SBS and the near-forward SBS that are generated in the droplet can emerge in the backward direction and enter the single-ended detection system.

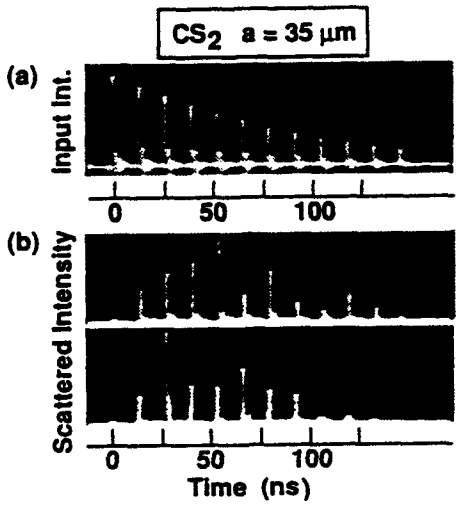

Figure 3. Time profile of (a) the green input-laser radiation and (b) the green scattered radiation from CS2 droplets. The pulse duration is 100 psec and the pulse interval is 13.2 nsec. A Pockel cell pulse selector passes 12 green input-laser pulses. The scattered intensities associated with the first and second input-laser pulses are always much weaker than the subsequent scattered pulses. [From Publication C].

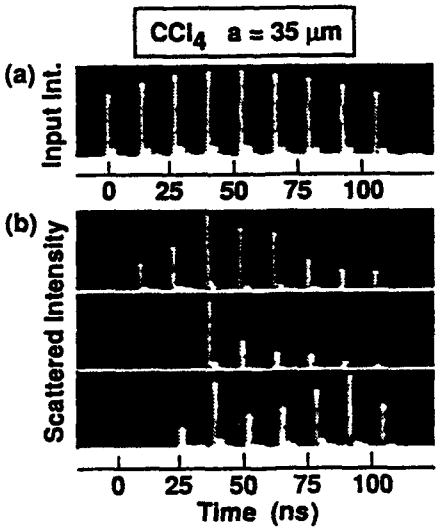

Figure 4. Time profiles of (a) the green input-laser radiation and (b) the green scattered radiation from CCl_4 droplets. [From Publication C].

(c) Stimulated Low-Frequency Scattering

During this ARO-funded grant period, we noted that the elastically-scattered and the SRS radiation are spectrally broadened towards the low frequency side of the input-laser line at ω_L and the SRS lines at ω_{js}, where j =1, 2, and 3. Figures 5 and 6 show the asymmetrical broadening extending continuously for more than 400 cm^{-1} from ω_L and ω_{js}. Such asymmetric broadening is only observed from liquids of highly anisotropic molecules, such as CS2, benzyl alcohol, toluene, and chloroform. Whereas stimulated light scattering associated with molecular vibrations (Raman, with discrete frequency shifts greater than 400 cm^{-1}) and acoustic waves (Brillouin, which discrete-frequency-shifts less than 0.2 cm^{-1}) in pure liquid droplets have been seen, an asymmetric and continuous spectral broadening has not been observed before.

Three physical processes affect the low-frequency shifts of the scattered light from liquids of anisotropic molecules: (1) Rayleigh wing scattering associated with diffusive reorientational motion; (2) librational scattering associated with angular oscillations of a molecule in a "cage" formed by inter-molecular interactions with neighboring molecules; and (3) dipole-induced-dipole scattering associated with inter-molecular interactions that result in translational motion of the molecules with respect to each other. We attribute our observations to multiple orders of stimulated librational scattering and to dipole-induced-dipole scattering. Stimulated Rayleigh wing scattering is ruled out because of the particular frequency spacing ($\approx$ 38 cm^{-1}) of the droplet MDR modes.

Similiar asymmetric broadening has been observed with a variety of pulses from the following input-lasers; (1) injection-seeded single-mode Q-switched laser of 7 nsec; (2) multimode Q-switched laser of 7 nsec; (3) a train of mode-locked pulses of 100 psec; and (4) excimer laser pumped dye laser of few cm^{-1} linewidth. We did not investigate such stimulated low-frequency scattering from pure water droplets nor water droplets containing anisotropic ions. However, we did observe asymmetric broadening of the C-H vibrational mode of ethanol droplets containing CS_2. [For more details see Publication D].

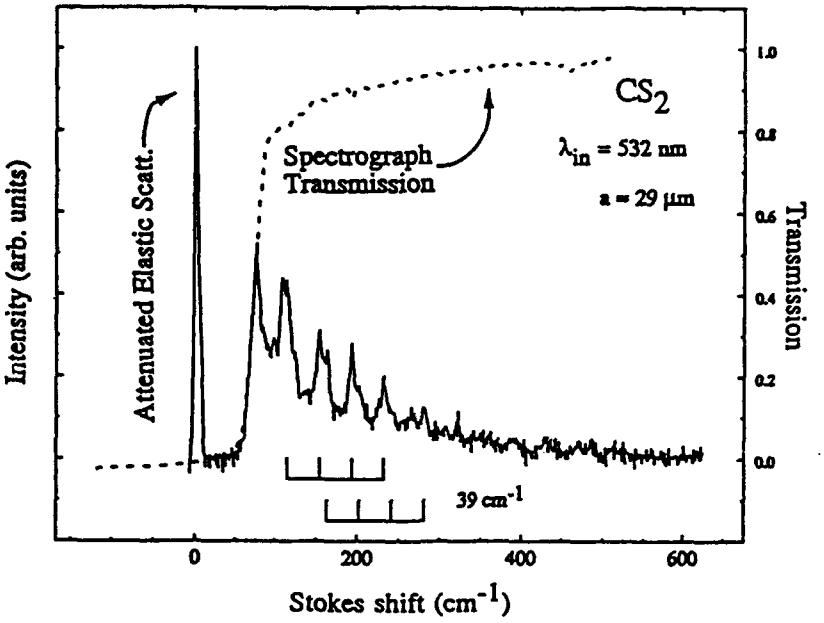

Figure 5. The stimulated low-frequency scattering (SLFS) spectrum from CS_2 droplets that extends to ≈ 400 cm^{-1} on the Stokes side (red wavelength side) of the input-laser frequency (designed with 0 cm^{-1} shift). The transmission of the triple-stage spectrograph is shown by a dotted curve. The elastic scattering of the input-laser radiation is greatly attenuated. The periodicity of the MDR peaks (39 cm^{-1}) is indicated. [From Publication D].

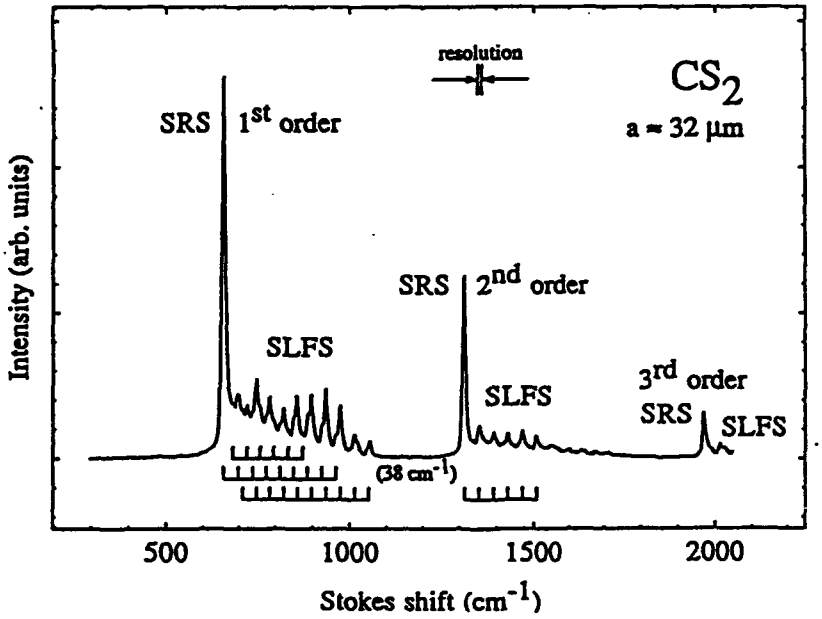

Figure 6. The SLFS spectrum from CS2 droplets that extends to ≈ 400 cm^{-1} on the Stokes side of each of the three-orders of SRS associated with the ν_1 mode of CS2 (with ω_{vib} = 656 cm^{-1}). The periodicity of the MDR peaks (38 cm^{-1}) is indicated. The spectral resolution of the spectrograph and linear-array photodiode detector is shown. [From Publication D].

(d) Resonance Raman Enhancement of SRS Gain

Resonance Raman scattering (RRS) refers to the enhancement of the Raman scattering when the photon energy of the incident light is nearly resonant or resonant with an electronic transition of a molecule. In the spontaneous light scattering regime (i.e., at low input intensity) the observation of RRS from fluorescent molecules is difficult because of the overwhelming amount of fluorescence produced. In fact, RRS spectra from highly fluorescent dyes such as the usual laser dye Rhodamine 6G, are difficult to obtain unless the fluorescence is reduced. The two standard techniques to reduce the fluorescence to an acceptable level for the detection of RRS spectra are as follows: (1) the use of surface enhanced RRS, where the Raman scattering is enhanced while the fluorescence is preferentially quenched by the metal; and (2) the use of Fourier-transform (FT) Raman scattering where the input-laser wavelength is in the near infrared and hence does not excite the fluorescence in the visible.

During the present ARO-funded grant period, we have demonstrated that stimulated resonance Raman scattering (SRRS) from microdroplet of 10^{-3} M Rhomdamine 6G dissolved in ethanol can be observed if the input-laser intensity is high enough. In order to achieve SRS from such a low concentration of solute (10^{-3} M Rhomdamine 6G), we took advantage of the fundamental difference between the lasing gain and the Raman gain. The lasing gain is always clamped at the threshold for lasing (i.e., a constant independent of the input intensity, I_{in}), and consequently the lasing output intensity is *linearly proportional* to I_{in}. By contrast, the stimulated Raman gain is proportional to I_{in}, and the saturation of the Raman gain is caused by the generation of multiorder SRS. Consequently, the first-order SRS output intensity is *exponentially proportional* to I_{in}. By increasing I_{in}, we were able to increase the stimulated Raman signal from R6G above and beyond the lasing signal from R6G.

Figure 7 shows the inelastic emission spectra from 10^{-3} M R6G. At low I_{in} (0.01 GW/cm^2), only the lasing emission can be observed. At medium I_{in} (0.1 GW/cm^2), the SRRS peaks (marked A, B, and C) become discernable from the lasing emission.

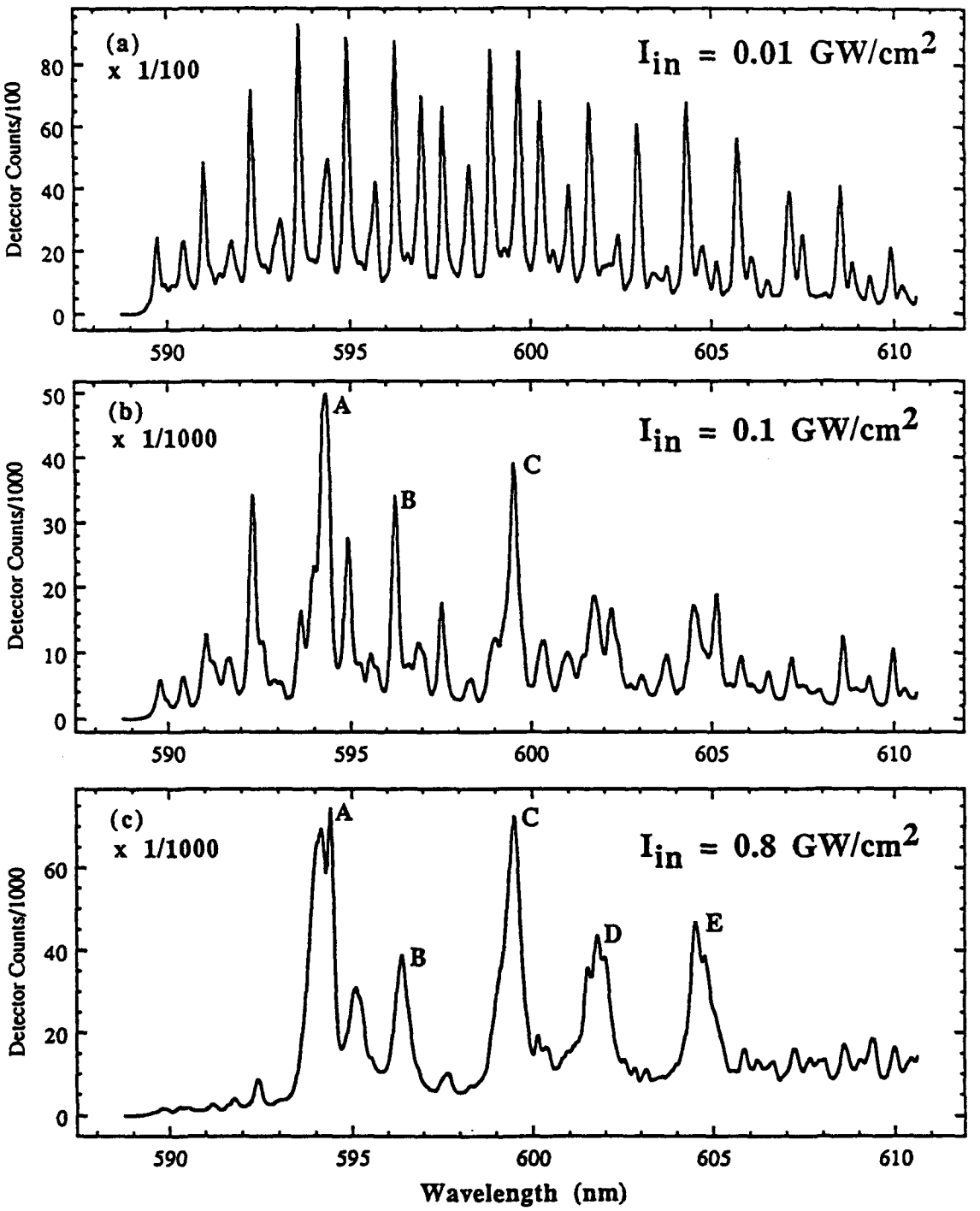

Figure 7. Inelastic emission spectra from 10^{-3} M R6G in ethanol droplets at three different I_{in}'s with the input laser wavelength at 550 nm. (a) At I_{in} = 0.01 GW/cm^2, the SRRS gain is low and only lasing can be observed. (b) At I_{in} = 0.1 GW/cm^2, three Raman peaks (labelled A-C) of R6G can be identified. (c) At I_{in} = 0.8 GW/cm^2, two more SRRS peaks (labelled D and E) can be observed and the SRRS signal dominates the lasing signal. Note the change in scale for the detected intensity, and the decrease in the lasing to SRRS intensity ratio as I_{in} increases. [From Publication E].

At high I_{in} (0.81 GW/cm^2), the SRRS peaks (marked A, B, C, D, and E) are prominent and readily distinguishable from the lasing spectra. [For more details see Publication E]. Without resonance Raman enhancement of the Raman gain, the lowest concentration of a minority species in a host liquid droplet that SRS can be achieved is about 1 M, (e.g., 1 M of NO_3^- in water droplets). Thus, we were pleased that with resonance Raman enhancement we were able to extend the lowest concentration of a minority species (R6G) to 10^{-3} M. We are not sure if the SRRS technique can be extended to trace detection in the parts-per-million range. Furthermore, we are not sure whether or not we can generalize these results with laser dyes in the visible wavelength region to trace species detection in the UV region.

(e) Extra Lasing Gain for SRS

While we were investigating stimulated resonance Raman scattering of Rhodamine 6G (R6G), we noted that as I_{in} is increased, the lasing emission signal actually decreased while the SRS signal increased, albeit not exponentially (see Fig. 7). The partial suppression of the R6G-lasing occurs when the discrete wavelength of the host-liquid SRS is within the broad spectral profile of the lasing emission. Because the SRS frequency is a constant difference from the input-laser frequency, $\omega_{SRS} = \omega_L - \omega_{vib}$, the discrete Raman wavelength can be judiciously selected by using λ_L from a tunable dye laser. By contrast, the broad emission profile of the lasing emission is independent of the pumping wavelength, so long as λ_L is in the absorption region of the dye molecule. When the discrete SRS wavelength overlaps with the broad lasing profile, the SRS photon stimulated radiative transitions in the population-inverted dye, and hence, provide "extra" gain for that particular discrete Raman wavelength. However, the remaining population in the excited electronic level of the dye molecule is decreased as a result of the increased stimulation at the discrete Raman wavelength. Consequently, the laser emission from all the wavelengths other than at the discrete Raman wavelength decreases. The suppression of the lasing emission is not total because the Raman intensity takes time to grow from the spontaneous

Raman "noise," as well as from the fluorescence where both serve as seeds for the SRS process.[5] Before the stimulated radiative transition induced by the discrete Raman photons becomes dominant, lasing emission can occur, because the lasing threshold is much lower than the SRS threshold. Figure 8 shows the discrete SRS emission overlapping the lasing spectra of R6G. The lasing intensity with $I_{in} = 0.8$ GW/cm^2 is less than that with a lower input-laser intensity, at $I_{in} = 0.4$ GW/cm^2. The SRS peak becomes distinct at $I_{in} = 0.8$ GW/cm^2. [For more details see Publication F].

We are just beginning to understand the interrelated roles of these three process (1) fluorescence seeding that is added to the spontaneous Raman "noise" in initiating the stimulated Raman scattering; (2) resonance enhancement of the Raman scattering cross-section and hence, the stimulated Raman gain when λ_L in in the electronic absorption band of the Raman molecule; and (3) extra Raman gain that is provided by the inverted population of the dye molecule when the discrete Raman scattering wavelength overlaps the lasing emission profile. Without any of these three processes, SRS generation of minority species concentration in water droplets[6] requires the species concentration to be ≈ 1 M. We are not decided as to whether or not there is a need for all three processes [(1) - (3)] to be operative before SRS generation of traces species in water droplets can be reached for concentrations in the 1-10 ppm level. The technique is too restrictive if all three processes are needed. We are presently attempting to determine the minimum detectivity level needed for SRS generation when only fluorescence seeding [process (1)] is operative. Most organic molecules and amino acid molecules fluoresce when irradiated in the UV, so that it is easy to achieve both fluorescence seeding and resonance enhancement. The final project is to use the water droplet as an optical cavity and use the fluorescence of the trace molecules to seed the Raman signal and the resonant enhanced Raman gain of the trace molecule to provide the Raman amplification.

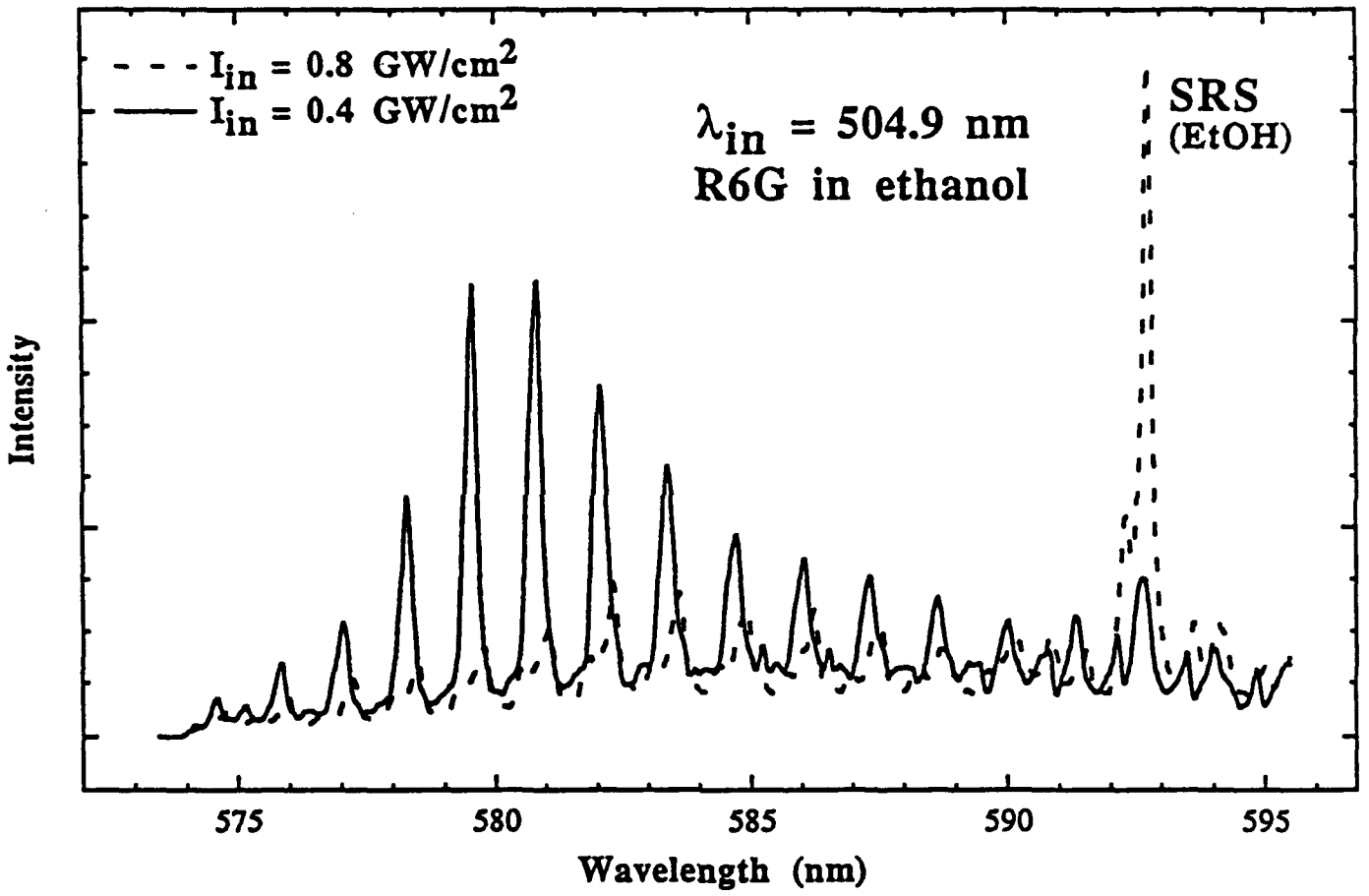

Figure 8. SRS and lasing spectra from R6G (1.25×10^{-4} M) ethanol droplets irradiated at two different input-laser intensities, I_{in} = 0.4 GW/cm^2 (solid curve) and I_{in} = 0.8 GW/cm^2 (dashed curve). The discrete SRS peak is labelled and the other peaks are associated with lasing of R6G. The input-laser wavelength is 504.9 nm. [From Publication F].

(f) Laser-Induced Radiation Leakage

Since all the research topics discussed above relied on the droplet as a high Q-factor optical cavity, we attempted to distinguish various possible perturbation mechansims that cause laser-induced "extra" radiation leakage from various locations on or within micrometer-sized droplets. Ray optics and Lorenz-Mie calculations of the internal and surface intensity distributions have shown that some of the input rays of a parallel plane wave, after refraction by the spherical illuminated face, converge toward a ring on the droplet shadow face. This ring of high surface intensity is referred to as the Descartes ring. The observation of laser-induced SRS leakage from the Descartes ring is significant because the extra emergence of SRS (other than tangentially from the rim of a perfect spherical droplet) has never been accounted for in the standard treatment of radiation leakage of nonlinear waves that is on a MDR. Along with the high intensity on the surface at the Descartes ring, there exist two internal regions of high intensity, just within the shadow face and the illuminated face, where the reflected and refracted rays can converge.

The possible mechanism for laser-induced radiation leakage from the Descartes ring on the droplet surface and from the localized regions within the droplet can be grouped in two categories. The first category is associated with elastic light scattering from the droplet surface and/or within the droplet as a result of inhomogeneous index of refraction. The second category is associated with surface bulging at the region of maximum surface intensity distribution.

We have attempted to isolate various laser-induced perturbation meachanisms that cause extra leakage of the internally generated dye-laser radiation. We purposely selected dye-lasing emission and not the SRS as the probe radiation. The dye-lasing threshold is much lower than the SRS threshold. Thus, we can avoid exposing the droplets to high-intensity laser pulses which are near the threshold for laser-induced plasma generation. Although much time was spent on this phase of the research, we were frustrated in not being able to ascribe the laser-induced perturbation to one of several possible mechanisms.

However, we did manage to clarify the importance of each of the possible mechanisms. For more details see Publication G].

(g) Goos-Hänchen Shift and Mode Spacing

The frequency spacing of MDR's with consecutive mode numbers provides a convenient measure of the droplet size. For very lossy MDRs (i.e., those MDR's with low Q-factor), there is an anomolous dependence of the frequency spacing with an increase of droplet radius. We attempted to use a ray picture to provide some physical explanation for this anomaly. For those lossy modes, the internal rays are envisioned to approach the liquid-air interface very near the critical angle for total internal reflection and hence, experience a large Goos-Hanchen shift which causes the effective radius of the droplet to be larger than the actual radius. Those rays that approach the droplet surface with an angle near the critical angle have a large Goos-Hänchen shift. The associated penetration depth is related to the decreased mode spacing. Goos-Hänchen shift is large when the penetration depth is significant and thus the round-trip optical pathlength increases. That is, the effective optical size of the spherical cavity is larger than its physical size for MDR's very near their cutoff frequencies. The smaller mode spacings would be expected to be based on the size parameter alone. We believe the inclusion of the Goos Hänchen shift and the associated penetration depth into the region outside the droplet surface helps in understanding the nature of those lossy (or low Q value) MDRs. [For details see Publication H].

(h) Review Papers

Two SPIE Conference Proceedings provided us opportunities to summarize our research results and to express our thoughts in a more tutorial manner, -- often discouraged in refereed articles. [For details see Publications I and J]. Nonlinear optical processes in micrometer-sized droplets were reviewed in a 1990 article by Chang and was dedicated to Professor Nicholaas Bloembergen's 70th birthday. Morphology-dependent resonances

which support nonlinear optical processes in droplets were reviewed by Hill in 1988. In 1992, the Proceedings of a Summer School on Nonlinear Optics in Denmark provided Steven C. Hill and me an opportunity to write a long review article that emphasizes the nonlinear optical phenomena and theory developed. [For details, see publication K]. Because nonlinear optical spectra contain information of the chemical species within the droplet and of the physical size and shape of the droplets, the nonlinear spectra can be used as an optical diagnostic technique for sprays. A review paper, intended for the combustion community, is submitted to the Recent Advances in Spray Combustion of the America Institute of Aeronautics and Astronautics. [For details see Publication L].

List of Publications that Acknowledged ARO DAALO3-91-G-0042

A. David H. Leach, Richard K. Chang, William P. Acker, and Steven C. Hill, "Third Order Sum Frequency Generation in Droplets: Experimental Results," JOSA B 10, 34 (1993).

B. Steven C. Hill, David H. Leach, and Richard K. Chang, "Third Order Sum Frequency Generation in Droplets: Model with Numerical Results for Third Harmonic Generation," JOSA B 10, 16 (1993).

C. Frederick H. Wirth, Kimberly A. Juvan, David H. Leach, J. Christian Swindal, Richard K. Chang, and P. T. Leung, "Phonon-Retention Effects on Stimulated Brillouin Scattering from Micrometer Droplets Illuminated with Multiple-Short Laser Pulses," Opt. Lett. 17, 1334 (1992).

D. Janice L. Cheung, Alfred S. Kwok, Kimberly A. Juvan, David H. Leach, and Richard K. Chang, "Stimulated Low-Frequency Emission from Anisotropic Molecules in Microdroplets," Chem. Phys. Lett. 213, 309 (1993).

E. Alfred S. Kwok and Richard K. Chang, "Stimulated Resonance Raman Scattering of Rhodamine 6G," Opt. Lett. 18, 1703 (1993)

F. Alfred S. Kwok and Richard K. Chang, "Suppression of Lasing by Stimulated Raman Scattering in Microdroplets," Opt. Lett. 18, 1597 (1993).

G. Gang Chen, Dipakbin Q. Chowdhury, Richard K. Chang, and Wen-Feng Hsieh, "Laser-Induced Radiation Leakage from Microdroplets," JOSA B 10, 620 (1993).

H. D. H. Leach, D. Q. Chowdhury, and R. K. Chang, "The Effect of Goos-Hanchen Shift on Geometrical Optics Model for Spherical Cavity Mode Spacing," J. Opt. Soc. Am. A., 11, 1110 (1994).

I. R.K. Chang, G. Chen, S.C. Hill, and P.W. Barber, "Nonlinear Optical Processes in Droplets with Single-Mode Laser Excitation", in Proceedings of the SPIE Conference on Nonlinear Optics and Materials, Vol. 1497 (SPIE, Bellingham, Washington, 1991), p. 2.

J. Steven C. Hill and Richard K. Chang, "On Modeling Nonlinear Optical Mixing Processes in Droplets," in Proceedings of the SPIE Conference on Laser Applications in Combustion and Combustion Diagnostics, Vol. 1862 (SPIE, Bellingham, Washington 1993), p. 309.

K. Steven C. Hill and Richard K. Chang, "Nonlinear Optics in Droplets," in Proceedings of the 5th International Topsøe Summer School on Nonlinear Optics (Aalborg, Denmark, 3-8 August, 1992) O. Keller, ed. Nova Science Publishers, New York, (in press).

L. J. Christian Swindal, G. Chen, A. Serpengüzel, R. K. Chang, and W. P. Acker "Spray Diagnostics with Lasing and Stimulated Raman Scattering," AIAA Progress Series "Recent Advances in Spray Combustion," American Institute of Aeronautics and Astronautics, Washington, D.C, (submitted).

List of Invited Talks at National and International Symposia:

(1) "Microcavity Characteristics Associated with a Single Liquid Droplet," Joint Meeting of Quantum Electronics and Laser Sciences (QELS) with Conference of Lasers and Electro-Optics (CLEO), Baltimore, MD, May 14, 1991 (Invited Talk).

(2) "Nonlinear Spectroscopy of Droplets," Annual Meeting of the Optical Society of America (OSA) and Meeting of Lasers and Electro-Optics Society (LEOS), San Jose, CA, November 5, 1991 (Invited Talk).

(3) "Stimulated Emission from Microdroplets" The Second Workshop on Quantum Optics, Weizmann Institute of Science, Rehovot, Israel, June 22-26, 1992. (Invited Talk).

(4 & 5) "Nonlinear Optical Effects in Micrometer Size Particles, I & II," 5th International Topsøe Summer School on Nonlinear Optics, Aalborg, Denmark, August 3-8, 1992. (Two Invited Talks).

(6) "Nonlinear Optical Processes in a Liquid Droplet Microcavity," 3rd International Conference on Electrical Transport and Optical Properties of Inhomogeneous Media, Guanajuato, Mexico, August 9-13, 1993. (Invited Talk).

(7) "Physical and Chemical Characterization of a Microdroplet from the Lasing Spectra," Annual Meeting of the Optical Society of America, Toronto, Canada, October 3-8, 1993. (Invited Lecture).

(8) "Determination of Flowing Droplet Properties from Stimulated Light Emission," International Aerosol Symposium, Karpov Institute, Moscow, Russia, March 21-25, 1994 (Invited Talk).

List of Plenary and Keynote Lectures at National and International Symposia.

(1) "Nonlinear Waves in Single Droplets," Optical Engineering Southcentral '91 Meeting on Nonlinear Optics and Materials of the Society for Photography and Image Engineering (SPIE), Dallas, TX, May 8, 1991 (Keynote Lecture).

(2) "Characteristics and Applications of Stimulated Raman Scattering in Microdroplets," XIIIth International Conference on Raman Spectroscopy, Würzburg, Germany, August 31-September 4, 1992. (Plenary Lecture).

(3) "Physical and Chemical Characterization of a Microdroplet from the Nonlinear Optical Spectra," 12th Annual Meeting of the America Association for Aerosol Research, Oak Brook, IL, October 11-15, 1993. (Plenary Lecture).

Students Awarded with Ph.D.

David H. Leach received his Ph.D. in May, 1991
Ali Serpengüzel received his Ph.D. in May, 1992
Alfred S. Kwok received his Ph.D. in May, 1993

Scientific Collaborators

William P. Acker, Texaco Research, Beacon, New York
Peter W. Barber, Professor, Clarkson University, Potsdam, New York
Gang Chen, Graduate student of Yale
Dipakbin Q. Chowdhury, Former Post-Doc Research Associate at Yale
Janice L. Cheung, Graduate student at Yale
Steven C. Hill, NRC Fellow at Atm. Sc. Lab., White Sands Missile Range, New Mexico
Wen-Feng Hsieh, Professor, Chiao-Tung University, Hsin-Chu, Taiwan
Kimberly A. Juvan, Former graduate student at Yale
Alfred S. Kwok, Former graduate student at Yale
David H. Leach, Former graduate at Yale
J. Christian Swindal, Graduate student at Yale
Frederick H. Wirth, Associate Professor, Hampshire College, Amherst, Massachusetts
Kenneth Young, Professor, Chinese University of Hong Kong

Report of Inventions

None